

Characterization of the ORBIT Indoor Testbed Radio Environment

Haris Kremo, Jing Lei, Ivan Šeškar, Larry Greenstein, and Predrag Spasojević
WINLAB, ECE Department, Rutgers University
Email: {harisk, michelle, seskar, ljg, spasojev}@winlab.rutgers.edu

Abstract—We perform a set of measurements of channel frequency responses at different points in the room that accommodates the ORBIT indoor testbed using a vector network analyzer (VNA). To validate the data collected with VNA we use spectrum analyzer (SA) measurements, as well. Four measurements are performed over non-overlapping 100 MHz bands in the industrial, scientific, and medical (ISM) band, and in the unlicensed national information infrastructure (UNII) band. The fifth measurement spans the coarsely sampled .4 to 6 GHz band. From the measured frequency responses we calculate path loss model parameters. The path loss exponent is between 1.1 and 2 and the dynamic range of the signal is around 25 dB across different bands. Based on the frequency responses measured over the .4 to 6 GHz band we determine multipath intensity profiles (MIP) with fine time granularity. The comparison of MIPs to the ray tracing simulations generated with WiSE software indicates that the surfaces perpendicular to the plane defined by the transmit and receive antennas represent a significant source of reflections. However, the reflections from the floor, dropped ceiling, and roof are suppressed by the antenna elevation patterns.

I. INTRODUCTION

ORBIT indoor testbed is the facility at WINLAB, Rutgers University, with 400 computers serving as network nodes, each of them equipped with two 802.11 a/b/g wireless interfaces [1]. ORBIT houses a smaller number of nodes with other types of interfaces, like MICA Motes and software defined GNU radios. The nodes are hanging from the ceiling at a distance of three feet from each other in a 20-by-20 rectangular grid.



Fig. 1. ORBIT indoor testbed

Propagation of radio waves in indoor environments has previously been studied for narrow band systems, as well as for wide band systems. An exhaustive tutorial on indoor propagation measurements and modeling is presented in [2]. The authors in [3] present 300,000 measurements of ultra-wide

band (UWB) indoor channel responses in urban and suburban houses, and describe a stochastic empirical path loss model for UWB channels. The same authors in [4] present delay profile models for indoor UWB channels, based on the same measurements. The technique of measuring channel frequency response using a vector network analyzer (VNA) is outlined in [5]–[7].

Radio environment modeling is the precursory step required to ensure repeatability and accuracy of the ORBIT experiments. The path loss model parameters, as well as the characterization of multipath, are necessary to provide isomorphic SNR-based mapping of different real-life wireless networking topologies on the testbed [8], [9]. Instead of the statistical approach to modeling, which is convenient for the characterization of a large number of similar environments like in [4], we use deterministic approach because we seek to establish a propagation model for a particular indoor environment. For that reason we measure the channel delay profile at a number of points in the ORBIT room. The dynamic range of the testbed signals is described by the path loss exponent and geometry (size) of the testbed.

Since radio devices deployed on the testbed use wide band modulation schemes we use the VNA to measure large number of complex responses across these wide bands. Rather than taking a painstaking geometric approach to detect the main sources of multipath, Wireless System Engineering (WiSE) software [10] allows us to compare the results of ray tracing with the measured delays of multipath components.

The rest of the paper is organized as follows. Section II outlines organization of measurements and presents hardware setup. In Section III are presented models for path loss and multipath intensity profiles. The results of measurements are presented in Section IV. Finally, Section V concludes the paper.

II. EXPERIMENTAL SETUP

Our measurements are organized in two case studies. The first case study involves 15 measurements in a straight line as in Fig. 2(a). The transmitter is fixed in the corner of the room. The receiver is moved along a straight line that stretches diagonally across the room and provides the line-of-sight (LOS) between the antennas. Both antennas are mounted at the height of 2.29 m, and using the same hardware as the antennas on the ORBIT nodes.

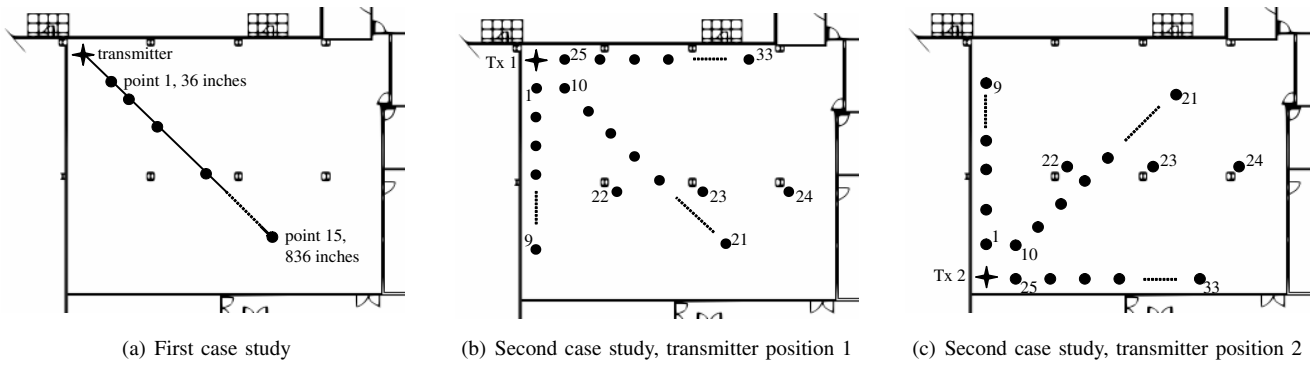


Fig. 2. Positions of the transmitter and receiver for both case studies

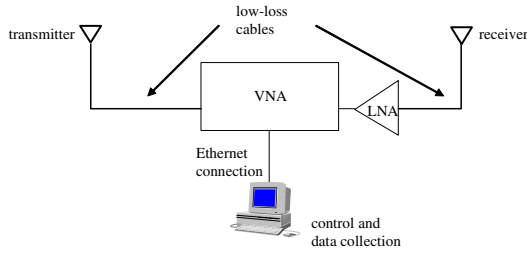


Fig. 3. Measurements setup with network analyzer

The second case study includes two transmitter positions and 66 receiver positions (33 for each transmitter position), as illustrated in Figs. 2(a) and 2(b). We removed two corner nodes and replaced their antennas with our transmit antenna. This setup emulates actual environment on the testbed since it considers the antennas on ORBIT nodes and their steel support as obstacles between the transmitter and the receiver. By deploying the transmit antenna at the corners we wanted to investigate whether the path loss model differs significantly for two spatially symmetric sets of measurements.

For both case studies the antennas were connected to the Agilent E5071B VNA with low-loss, double shielded, 60 feet cables, as in Fig 3. The cables have maximum loss of 6 dB at 6 GHz. We used HG2458RD-RSP Rubber Duck vertically polarized omni-directional antennas which are designed to operate within the industrial, scientific, and medical (ISM) band, and in the unlicensed national information infrastructure (UNII) band. The difference between the maximum and minimum gain of the antennas in the azimuthal plane is smaller than 3 dB [11]. Due to the fact that the transmitter and the receiver were at the same height, the elevation gain of the antennas was the same for all measurements. We used these antennas for coarsely sampled band as well, since “on-the-shelf” antennas for such huge bandwidth were not available to us. Interested reader is referred to [12] for more information on challenges in the design of UWB antennas. The signal at the receiver port of the VNA was amplified by a 36 dB low-noise wide band amplifier.

Within a two minute interval VNA cycles 10 times through five selected bands, sweeping each band every 12 seconds.

The VNA response corresponds to measurements at $J = 1601$ distinct tones over five bands. The first four bands are 100 MHz wide: 2.4 GHz to 2.5 GHz, 5.15 GHz to 5.25 GHz, 5.25 GHz to 5.35 GHz, and 5.725 GHz to 5.825 GHz. These bands are within ISM and UNII bands. The fifth, coarsely sampled band spans 400 MHz to 6 GHz. The VNA measures complex values of the scatter parameter S_{21} which corresponds to the channel frequency response $H(f, d, t)$. The channel frequency response is in general a function of the signal frequency f , distance between antennas d , and time t .

For the widest band the maximum excess delay is

$$\tau_{max} = \frac{1600}{6 \text{ GHz} - 0.4 \text{ GHz}} = 286 \text{ ns.}$$

This maximum delay corresponds to the maximum distance of 85.65 m, which is sufficient for the ORBIT room. The multipath resolution is determined by the inverse of the bandwidth

$$\Delta\tau = \frac{1}{6 \text{ GHz} - 0.4 \text{ GHz}} = 178.57 \text{ ps.}$$

This multipath resolution is sufficient to distinguish reflections with difference in path length of 5.35 cm.

The room was kept empty and as much as possible free from the interference of devices which operate in the same bands like 802.11 access points. Loss in cables and amplifier gain were extracted from the results by running the calibration measurement with short-connected cables. The measurements were automated and remotely controlled through a program written in C# language.

We paid special attention to the effects of the antenna elevation patterns on the measurements. In [13] is shown how changes in antenna gain, caused by differences in heights, result in the change of the path loss exponent.

A. Auxiliary Setup With Spectrum Analyzer

The auxiliary setup, shown in Fig. 4, with the signal generator (SG) and the spectrum analyzer (SA), was used to verify the measurements collected using VNA for the first case study. The measurements were repeated at the same points as for the VNA, but only over four 100 MHz bands. In each of the 100 MHz bands we collected $J = 51$ measurements of signal strength.

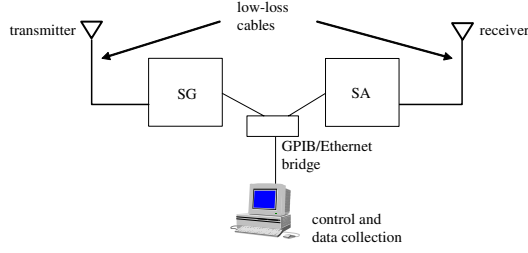


Fig. 4. Measurements setup with spectrum analyzer

III. THEORETICAL BACKGROUND

A. Path Loss

Path loss is typically modeled by (1), where $PL(d)$ represents path loss in dB at distance d from the transmitter, γ represents path loss exponent, PL_1 is path loss at reference distance d_1 , and S is a log-normal, zero-mean random variable with variance σ dB [3].

$$PL(d) = PL_1 + 10\gamma \log_{10} \left(\frac{d}{d_1} \right) + S \quad (1)$$

Let $H_i(f_j, d_k)$ denote one of 10 channel responses recorded during a two-minute experiment at k -th point in space, $k = 1, 2, \dots, K$, and over a frequency f_j , $j = 0, 1, \dots, J-1$, in a bandwidth $f_{J-1} - f_0$. We first perform time averaging of the channel response

$$H(f_j, d_k) = \frac{1}{10} \sum_{i=1}^{10} H_i(f_j, d_k). \quad (2)$$

The path loss in dB, at point k , is given by

$$PL(d_k) = -10 \log_{10} \left[\frac{1}{J} \sum_{j=0}^{J-1} |H(f_j, d_k)|^2 \right]. \quad (3)$$

The path loss exponent γ^* and the path loss at the reference distance PL_1^* are determined as

$$(\gamma^*, PL_1^*) = \arg \min_{\gamma, PL_1} \left\{ \sum_{k=1}^K [PL(d_k) - PL_{fit}(d_k; \gamma, PL_1)]^2 \right\} \quad (4)$$

where

$$PL_{fit}(d; \gamma, PL_1) = PL_1 + 10\gamma \log_{10} \left(\frac{d}{d_1} \right).$$

B. Multipath Intensity Profile

Complex channel impulse response $\{a_j^k\}$ is the inverse discrete Fourier transform of $H(f_j, d_k)$. The multipath intensity profile (MIP) [4] at distance d_k is then

$$p^k(\tau) = \sum_{j=0}^{J-1} p_j^k(\tau) \delta(\tau - j\Delta\tau), \quad (5)$$

where

$$p_j^k = \frac{|a_j^k|^2}{\sum_{j=0}^{J-1} |a_j^k|^2}$$

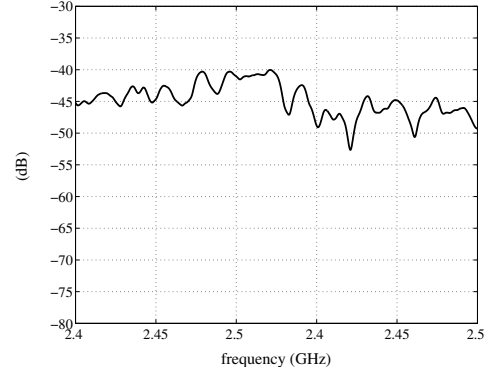


Fig. 5. An example of channel response $|H(f_j, d_k)|$ measured with VNA for the second case study across 2.4 GHz to 2.5 GHz band

TABLE I

PATH LOSS PARAMETERS FOR THE FIRST CASE STUDY

band (GHz)	VNA		SG and SA	
	γ^*	PL_1^*	γ^*	PL_1^*
2.4 to 2.5	1.638	-44.972	1.847	-42.202
5.15 to 5.25	1.683	-48.335	1.583	-48.106
5.25 to 5.35	1.645	-49.116	1.601	-50.501
5.725 to 5.825	1.162	-56.017	1.138	-55.728
0.4 to 6	1.730	-49.592		

represents the normalized power of the j -th component of the impulse response.

IV. RESULTS

Fig. 5 shows an example of the magnitudes of measured channel response $|H(f_j, d_k)|$ for the second case study, transmitter position 1, and point 11.

A. Path Loss Modeling

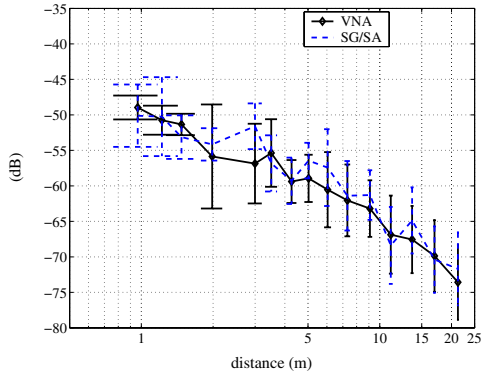
Fig. 6(a) shows path loss values calculated from (3) for the first case study in 5.15 GHz to 5.25 GHz band. The bars represent standard deviation limits. The standard deviation is calculated from the collected J power measurements in linear scale and then converted to dB. The loss values $PL(d_k)$, $k = 1, 2, \dots, 15$, calculated from (4), are presented in Fig. 6(b). In this figure the path loss models are compared to the values calculated using Friis free space equation [14] for 5.2 GHz

$$PL(d) = 20 \log_{10} \left(\frac{4\pi df}{c} \right), \quad (6)$$

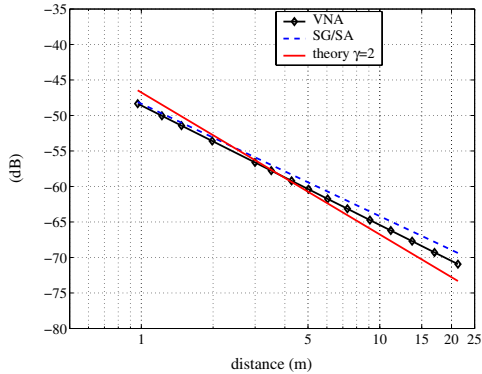
where c represents the speed of light in the vacuum.

Table I summarizes results for the first case study. Except for the values measured in 5.725 GHz to 5.825 GHz band, the path loss exponents are smaller, but close to two. Such results are typical for almost empty indoor environments [2]. In the 5.725 GHz to 5.825 GHz band, the path loss exponent is close to unity both for the setup with the VNA, and for the setup with SA. Reference [2] lists several examples of a path loss coefficient somewhat larger than one in large rooms or halls.

As an example of results for the second study, Fig. 7(a) presents measured path loss parameters in 2.4 GHz to 2.5 GHz band. Fig. 7(b) contains path loss models for both transmitter

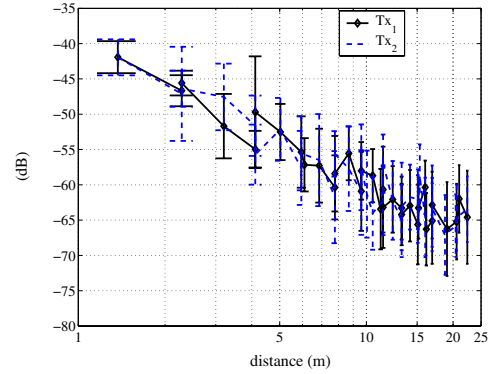


(a) Case study 1, measured path loss

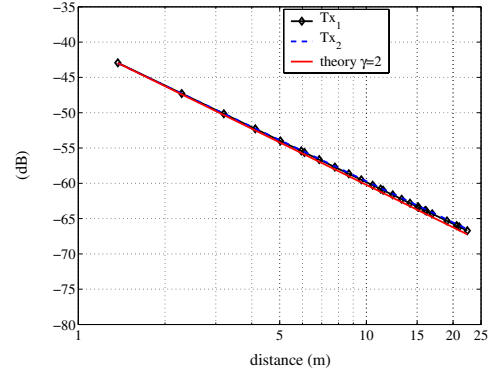


(b) Case study 1, modeled path loss

Fig. 6. Measured and modeled path loss for the first case study across 5.15 GHz to 5.25 GHz



(a) Case study 2, measured path loss



(b) Case study 2, modeled path loss

Fig. 7. Measured and modeled path loss for the second case study across 2.4 GHz to 2.5 GHz

TABLE II

PATH LOSS PARAMETERS FOR THE SECOND CASE STUDY

band (GHz)	transmitter position 1		transmitter position 2	
	γ^*	PL_1^*	γ^*	PL_1^*
2.4 to 2.5	1.960	-42.934	1.937	-42.993
5.15 to 5.25	1.660	-54.459	1.701	-53.164
5.25 to 5.35	1.718	-53.411	1.706	-52.805
5.725 to 5.825	1.732	-53.398	1.902	-50.963
0.4 to 6	1.821	-50.623	1.833	-49.615

positions compared to free space loss at 2.45 GHz. The dynamic range of the signal across these distances is around 25 dB.

Table II summarizes results for the second case study. Depending on the band and the transmitter position, the path loss exponent varies between 1.66 and 1.96. Both the path loss exponent γ and the path loss at reference distance PL_1 show remarkable closeness over different transmitter positions.

B. Multipath Intensity Profiles

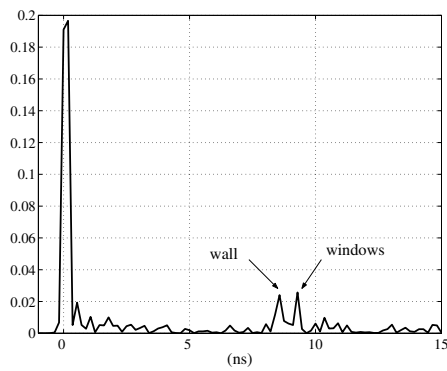
Fig. 8 presents an example of multipath intensity profile from the first case study. The profile is normalized with respect to time axis by setting the delay of the LOS component to zero. The figure shows strong reflections that originate from large surfaces perpendicular to the horizontal plane defined by the positions of the transmit and receive antennas. On the other hand, the reflections from the dropped ceiling, the roof, and

the floor, although predicted by WiSE, are not present. This effect is caused by the antenna elevation pattern. We measured the elevation pattern at 6 frequencies separated by 20 MHz, starting at 2.4 GHz up to 2.5 GHz. The average is presented in Fig. 9(b) and it indicates that in this band the antenna gain in directions toward the floor can be significantly smaller than the gain in the horizontal plane. To illustrate this effect in more detail for the 400 MHz to 6 GHz band, we measured the impulse response for the transmitter and the receiver separated by 2.48 m with the antennas tilted by 45° so that the point on the floor half a distance between the antennas belongs to the intersection of the planes perpendicular to the antenna orientation. The antennas are positioned at 1.24 m (a half of the separation distance) from the floor. In the Fig. 9(a) the reflection from the floor exactly matches the delay predicted by WiSE.

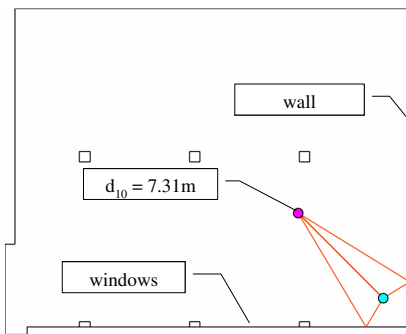
V. CONCLUSION

We performed a set of measurements of radio channel responses across different bands in the room that accommodates the ORBIT indoor testbed. From measured channel responses we evaluated the path loss model. We have also determined multipath intensity profiles at a number of points in the ORBIT room.

The measured path loss exponent for different bands and different transmitter positions is between 1.1 and 2. The dynamic



(a) MIP at point 10



(b) WiSE model at point 10

Fig. 8. Example of measured MIP. Delays of the strongest reflections are compared to the WiSE prediction.

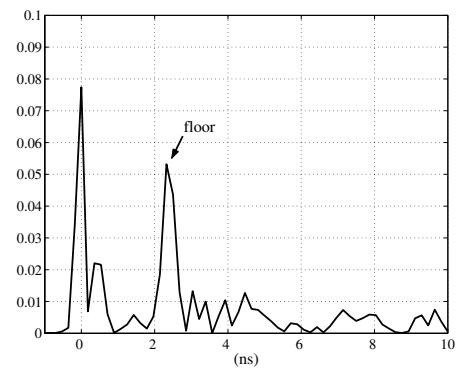
range of the signal is around 25 dB across different bands. We compared measured multipath intensity profiles with the predictions calculated by WiSE. Both the measurements and the simulations indicate that the large surfaces perpendicular to the plane defined by the transmit and receive antennas represent significant source of reflections. The measured reflections from the floor, dropped ceiling, and roof are suppressed by the antenna elevation patterns.

ACKNOWLEDGMENT

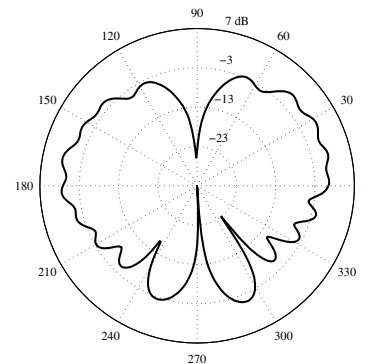
We would like to thank Ilya Korisch from Lucent Technologies in Holmdel for his help in characterizing antennas we used for the measurements.

REFERENCES

- [1] D. Raychaudhuri, I. Seskar, M. Ott, S. Ganu, K. Ramachandran, H. Kremono, R. Siracusa, H. Liu, and M. Singh, "Overview of the ORBIT radio grid testbed for evaluation of next-generation wireless network protocols," *IEEE Wireless Communications and Networking Conference*, March 2005.
- [2] H. Hashemi, "Impulse response modeling of indoor radio propagation channels," *IEEE Journal on Selected Areas in Communications*, vol. 11, no. 7, pp. 967–978, September 1993.
- [3] S. S. Ghassemzadeh, L. J. Greenstein, A. Kavcic, T. Sveinsson, and V. Tarokh, "An empirical indoor path loss model for ultra-wideband channels," *Journal of Communication and Networks*, no. 5, pp. 303–308, 2003.
- [4] S. S. Ghassemzadeh, L. J. Greenstein, T. Sveinsson, A. Kavcic, and V. Tarokh, "UWB delay profile models for residential and commercial indoor environments," *IEEE Transactions on Vehicular Technology*, vol. 54, no. 4, pp. 1235–1244, July 2005.



(a) MIP with antennas tilted by 45°



(b) Antenna elevation pattern between 2.4 GHz and 2.5 GHz

Fig. 9. Effect of the antenna elevation pattern on impulse response. As the antennas are tilted by 45° from the vertical direction the reflection from the floor becomes significant.

- [5] S. J. Howard and K. Pahlavan, "Measurement and analysis of the indoor radio channel in the frequency domain," *IEEE Transactions on Instrumentation and Measurements*, vol. 39, no. 5, pp. 751–755, October 1990.
- [6] H. Zaghoul, G. Morrison, and M. Fattouche, "Frequency response and path loss measurements of indoor channel," *Electronic Letters*, vol. 27, no. 12, pp. 1021–1022, June 1991.
- [7] A. M. Street, L. Lukama, and D. J. Edwards, "Use of VNAs for wide-band propagation measurements," *IEE Proceedings on Communications*, vol. 148, no. 6, pp. 411–415, December 2001.
- [8] J. Lei, R. Yates, L. Greenstein, and H. Liu, "Wireless link SNR mapping onto an indoor testbed," *First International Conference on Testbeds and Research Infrastructures for the Development of Networks and Communities*, Trento, Italy, February 2005.
- [9] —, "Mapping link SNRs of wireless mesh networks onto an indoor testbed," *TRIDENTCOM '06*, March 2006.
- [10] S. Fortune, D. Gay, B. Kernighan, O. Landron, R. Valenzuela, and M. Wright, "WiSE design of indoor wireless systems: practical computation and optimization," *IEEE Computational Science and Engineering*, vol. 2, no. 1, pp. 58–68, Spring 1995.
- [11] *2.4 GHz to 5.8 GHz 3 dBi Reverse Polarity-SMA TriBand Rubber Duck Wireless LAN Antenna: Model HG2458RD-RSP*, HyperLink Technologies, Inc. [Online]. Available: www.hyperlinktech.com
- [12] G. Lu, S. von der Mark, I. Korisch, L. Greenstein, and P. Spasojevic, "Diamond and rounded diamond antennas for ultrawide-band communications," *IEEE Antennas and Wireless Propagation Letters*, vol. 3, no. 1, pp. 249–252, 2004.
- [13] G. Santella and E. Restuccia, "Analysis of frequency domain wide-band measurements of the indoor radio channel at 1, 5.5, 10 and 18 GHz," *GLOBECOM '96*, vol. 2, November 1996, pp. 1162–1166.
- [14] T. S. Rappaport, *Wireless Communications: Principles and Practice*. Prentice Hall PTR, 2001.